Received: 4 November 2021 | Accepted: 4 January 2022

DOI: 10.1111/1759-7714.14324

ORIGINAL ARTICLE

WILEY

Recruitment of IL-1β-producing intermediate monocytes enhanced by C5a contributes to the development of malignant pleural effusion

Lisha Luo[1] | Shuanglinzi Deng[1] | Wei Tang[1] | Xinyue Hu[1] | Feifei Yin[1] | Huan Ge[1] | Jiale Tang[2] | Zhonghua Liao[2] | Xiaozhao Li[2] | Juntao Feng[1]

[1]Department of Respiratory Medicine, Key Cite of National Clinical Research Center for Respiratory Disease, Xiangya Hospital, Central South University, Changsha, China

[2]Department of Nephrology, Xiangya Hospital, Central South University, Changsha, China

Correspondence
Juntao Feng, Juntao Feng, Department of Respiratory Medicine, Key Cite of National Clinical Research Center for Respiratory Disease, Xiangya Hospital, Central South University, Changsha, Hunan 410008, China.
Email: jtfeng1976@csu.edu.cn

Xiaozhao Li, Department of Nephrology, Xiangya Hospital, Central South University, Changsha, Hunan 410008, China.
Email: lixiaozhao@csu.edu.cn

Funding information
Clinical Medical Technology Innovation Guidance Program of Hunan Province, Grant/Award Number: 2020SK53701; Natural Science Foundation of Hunan Province, Grant/Award Number: 2020JJ4887; The Key Research and Development Program of Hunan Province, Grant/Award Number: 2021SK2033

Abstract

Background: Monocytes are involved in tumor growth and metastasis, but the distribution of monocyte phenotypes and their role in the development of malignant pleural effusion (MPE) remains unknown.

Methods: A total of 94 MPE patients (76 diagnosed with adenocarcinoma lung cancer and 18 with squamous cell lung cancer) and 102 volunteers for health examination in Xiangya Hospital from December 2016 to December 2019 were included in the study.

Results: The distribution of monocyte subtypes identified by the expression of CD14 and CD16 were analyzed by flow cytometry. The proportion of $CD14^{++}CD16^{+}$ intermediate monocytes were significantly increased in pleural effusion of MPE patients. The complement system components were assayed by immunohistochemistry and ELISA, and higher expression of the classical and alternative pathways were detected in malignant pleural tissue. Transwell assay further revealed that C5a enhanced the infiltration of intermediate monocytes into the pleural cavity by promoting CCL2 production in pleural mesothelial cells (PMCs). In addition, C5a promoted the secretion of IL-1β by intermediate monocytes. Furthermore, C5a activated in intermediate monocytes and IL-1β released after C5a stimulation by monocytes promoted the proliferation, migration, adhesion, and epithelial-to-mesenchymal transition (EMT) of tumor cells, and attenuated tumor cell apoptosis.

Conclusions: C5a, activated by the classical and alternative pathways of the complement system, not only mediated the infiltration of intermediate monocytes by enhancing CCL2 production in PMCs but also induced IL-1β release from the recruited monocytes in MPE. The consequence of C5a activation and the subsequent IL-1β overexpression in intermediate monocytes contributed to MPE progression.

KEYWORDS
A549, C5a, IL-1β, malignant pleural effusion, monocytes

INTRODUCTION

Malignant pleural effusion (MPE) is a common and disabling complication of cancer, with one-sixth of patients with malignancy reported to develop effusions during the course of disease.[1] Approximately 75% of pleural malignancies are caused by lung cancer, breast cancer, or leukemia.[2] As the second most common exudative pleural effusion, however, very little information is available on the immune mechanisms involved in the development of MPE. Previous studies have shown an increased number of $CD4^{+}$ helper T lymphocytes in MPE, and further revealed that the underlying mechanism is

inflammatory cytokines and chemokines which mediate the differentiation and recruitment of $CD4^+$ T cell subtypes in the pleural cavity.[3–5] As effector cells of innate immunity, $CD14^+$ monocytes are associated with an inadequate response to chemotherapy in small cell lung cancer.[6] In squamous cell lung cancer, the infiltrated monocytes highly express factor XIIIA, which promotes lung cancer cell invasion and metastasis.[7] However, the role of monocytes in the development of MPE has not previously been investigated.

Human blood monocytes are broadly classified into three subsets: "classical" $CD14^{++}CD16^-$ monocytes responding to CCL2 and CCL7, which signal through CCR2; "nonclassical" $CD14^+CD16^+$ monocytes expressing CX3CR1, which pairs with CX3CL1; and "intermediate" $CD14^{++}CD16^+$ monocytes which share the features of both classical and nonclassical monocytes and express CCL2, CCL7 and CX3CL1.[8] Chemokines binding to their receptors can induce the recruitment of monocytes to sites of infection. It has been well documented that an accumulation of monocytes is associated with poor prognosis in cancer,[6,7] but the subtype distribution and mechanism of infiltrated monocytes subtype in MPE are poorly elucidated.

As a modulator and effector of innate immune responses, complement activation not only provides protection against pathogens but also participates in tumorigenesis.[9] Complement activation via the classical, lectin, and alternative pathways generates multiple effector molecules, including C5a, which induces monocyte and neutrophil chemoattraction and activation by binding to C5aR.[10,11] Complement activation has been implicated as a driver of tumor growth and metastasis in the tumor microenvironment.[12] The expressions of C3, C5, C1q, and factor H are increased in lung and breast cancer.[13–16] C5a is involved in tumor immune mechanisms and promotes tumor cell growth in solid tumors, such as lung, colon, and breast tumors.[17] Blockade of the C5a-C5aR1 axis can impair lung cancer bone metastasis and the growth of gastric cancer in mice.[18,19] Additionally, C5a has been reported to induce A549 cell proliferation, which plays a vital role in the development of lung cancer.[20] However, little is known about whether the activation of the complement system, especially C5a, is involved in the development of MPE.

Our previous study found that complement effector C5a not only enhanced the activation of nonclassical monocytes through cytokine release (IL-1β, IL-17 and IL-27), but also promoted the recruitment of nonclassical monocytes to the pleural cavity through CCL2, CCL7 and CX3CL1.[21] However, the relationship between C5a and monocytes in MPE is still unclear. In this study, we explored the distribution and phenotypic characteristics of monocytes, the activation of the complement pathway, the possible mechanism of monocyte recruitment into the pleural space, and the potential role of C5a and IL-1β-producing intermediate monocytes in the development of MPE.

Overall, we demonstrated that C5a promoted the infiltration of intermediate monocytes to the pleural space by enhancing CCL2 production in PMCs. C5a also induced IL-1β release from the recruited monocytes. The accumulated C5a and IL-1β in MPE promoted the proliferation, apoptosis, migration, invasion, and epithelial-to-mesenchymal transition (EMT) of lung cancer cells, which contributes to the development of MPE.

METHODS

Subjects

The study protocol was approved by the Ethics Committee of Xiangya Hospital, Changsha, China. All the enrolled patients signed informed consent forms. A total of 94 MPE patients (76 diagnosed with adenocarcinoma lung cancer and 18 with squamous cell lung cancer) and 102 volunteers for health examination in Xiangya Hospital from December 2016 to December 2019 were included and are summarized in Table S1. In follow-up in vitro experiments, the clinical characteristics of 16 patients from the MPE group, and 16 heart failure patients with transudate pleural effusion are summarized in Table S2.

All MPE patients were evidenced by the demonstration of malignant cells in the pleural fluid and/or on closed pleural biopsy specimen. Heart failure diagnosis was confirmed according to the European Society of Cardiology (ESC) guidelines by clinical examination, medical history, and echocardiographic examination by one of four experienced cardiologists. At the time of sample collection, none of the patients had received any anticancer therapy, corticosteroids, other nonsteroidal anti-inflammatory drugs or received any invasive procedures of the pleural cavity within 3 months before hospitalization. None of the patients had any history of carcinoma or pulmonary infection within 1 month prior to hospitalization.

Cells and reagents

Lung adenocarcinoma cell lines A549 obtained from the American Type Culture Collection (ATCC) were cultured in RPMI-1640 medium with 10% fetal bovine serum at 37°C, 5% CO_2. The reagents for *in vitro* cell treatment are listed in Table S3.

Immunohistochemistry

Four micrometers of formaldehyde-fixed pleural tissue were dewaxed and rehydrated with an alcohol gradient and PBS. Antigen retrieval was performed with citrate (pH 6.0). Endogenous peroxidase was blocked with 3% H_2O_2 in water for 20 min, and nonspecific binding was blocked with diluted normal goat serum for 60 min, and was then incubated with the primary antibody (mouse anti-human monoclonal antibody C1q (ab71089), rabbit anti-human polyclonal antibody factor B (ab192577), rabbit anti-human

polyclonal antibody factor P (ab186834), mouse anti-human monoclonal antibody MBL (ab23457), mouse anti-human monoclonal antibody factor H (ab118820), mouse anti-human monoclonal antibody C3a (ab37230), mouse anti-human monoclonal antibody C5a (ab11877) and rabbit anti-human polyclonal antibody SC5b-9(ab55811), all antibodies were purchased from Abcam) for 18 h at 4°C. According to the manufacturer's instructions, labeling was identified using the SP goat IgG kit (PV-6000, ZSGB-Bio, China). The chromogenic reaction solution contained 3, 3′-diaminobenzidine (DAB) (ZLI-9018, ZSGB-Bio, China), and counterstaining was performed with Mayer's hematoxylin (Solarbio). Slides were viewed under an imaging fluorescence microscope (Olympus BX51; Olympus).

Immunofluorescence staining

The slides of cells were embedded in paraffin according to standard pathology protocols. After antigen retrieval and permeabilization with 0.3% Triton X-100, tissues were incubated incubated at 4°C overnight with the recommended concentrations of primary Abs (mouse anti-human antibodies, including C5a (ab11877, Abcam), CCL2 (MABN712, Millipore), and rabbit anti-human antibodies, such as C5aR1 (ab59390, Abcam), CCR2(NBP1-48337, Novusbio)) by the manufacturer. After washing, slides were incubated with selected secondary Abs (AF594- goat anti-mouse IgG (ab150116, Abcam), AF488- goat anti-rabbit IgG (ab150077, Abcam), AF647- donkey anti-goat IgG (ab150131, Abcam)) for 40 min at room temperature in the dark, correctly matched to the appropriate species. DAPI mounting medium (Vector Laboratories) was used for cell nuclei staining. Finally, slides were viewed under an imaging fluorescence microscope (Olympus BX51; Olympus).

Flow cytometry

The expression markers on monocytes from MPE and blood were determined by flow cytometry as previously described.[21] The expression markers on monocytes from MPE and blood were determined by flow cytometry after surface staining with APC-Cy7 mouse anti-human CD45 mAb, FITC mouse anti-human CD14 mAb, and PE-Cy7 mouse anti-human CD16 mAb (BD Biosciences). Flow cytometry was performed on a BD FACS CantoII flow cytometer using Flowjow 10.0 software.

Cell isolation

Peripheral blood and pleural effusion were collected and overlaid on Ficoll Paque-PLUS (GE Healthcare) and centrifuged at 800 *g* for 10 min. The peripheral blood mononuclear cells (PBMCs) or pleural effusion mononuclear cells (PFMCs) at the interface of plasma and Ficoll were isolated. Mononuclear cells were identified in the singlets gate (FSC-A/FSC-H). Monocytes were identified within the SSC-A^{hi} $CD45^{+}$ cells and gated for the $CD14^{++}CD16^{-}$, $CD14^{+}CD16^{+}$ and $CD14^{++}CD16^{+}$ subsets. $CD14^{++}CD16^{+}$ monocytes from PBMC or PFMCs were sorted by BD FACS Aria II (BD Biosciences). After sorting, CD14 and CD16 expression on isolated cells were analyzed by flow cytometry (Figure S1). Isolated monocytes were incubated in RPMI 1640 (Gibco, Invitrogen) containing 10% heat-inactivated fetal bovine serum (FBS, Gibco) at 37°C in 5% CO_2.

For isolating PMCs, the cell pellets of MPE were resuspended in DMEM (Gibco, Invitrogen) containing 20% heat-inactivated fetal bovine serum (FBS, Gibco). The cells were seeded into 75 cm^2 flasks at a density of 1×10^4 cells/cm^2 and placed in an incubator at in 37°C 5% CO_2. After 24 h, the monolayers were washed with PBS to remove non-adherent cells, and fresh media was added. The monolayers were monitored until confluent (7–10 days), trypsinized, and subcultured for five to six passages.

PCR

The lysis of intermediate monocytes in MPE and transudate pleural effusion were collected and measured by real-time qPCR. Total RNAs were extracted from cells with TRIzol reagent (Invitrogen). The levels of mRNA were quantified by quantitative reverse transcription PCR (RT-qPCR) using SYBR Green (Takara), with GAPDH as internal normalized references. The RT-qPCR results were analyzed and are shown as relative mRNA levels of the CT (cycle threshold) values, which were then converted as fold change. Primers are listed in Table S4.

ELISA

The concentrations of complement component, chemokines and cytokines in pleural fluids and culture supernatant were collected and measured by ELISA kits according to the manufacturers' protocols (all kits were purchased from Raybiotech, Ebioscience and Elabscience).

Western blot assay

Western blot assay was conducted as previously described.[22] Briefly, cells were lysed with RIPA lysis buffer (Servicebio, China) plus 1 mmol/l phenylmethanesulfonyl fluoride (PMSF) (Servicebio, China) for 30 min. The homogenates were centrifuged at 15 000 × *g* for 15 min at 4°C. Equal amounts of protein were subjected to 10% sodium dodecyl sulfate-polyacrylamide gel electrophoresis. After transferring, membranes were blocked with 5% nonfat dry milk or 5% bovin serum albumin (for phosphorylated proteins) for 1 h and then incubated at 4°C overnight with primary antibodies (Table S5) followed by incubation with horseradish

peroxidase-conjugated secondary antibodies for 1 h at room temperature. The bands were detected using the Image Lab system.

Monocyte chemotaxis assays

The 8-μm pore polycarbonate filters in 24-well transwell chambers (Corning Costar) were used to perform the migration assay. Purified monocytes from blood (2×10^5) were added into the top chamber resuspended in RPMI 1640 medium in the final volume of 100 μl, supernatants of PMCs were placed in the bottom chamber in a volume of 600 μl, and the chambers were incubated at 37°C in 5% CO_2 atmosphere for 3 h. Finally, the nonmigratory cells in the upper chamber were scraped off and washed gently in PBS. The migratory cells on the bottom surface of the transwell membrane were fixed in 4% paraformaldehyde for 10 min and then underwent Wright-staining, before being viewed and photographed under a digital microscope (Olympus BX51; Olympus). The chemotaxis index was calculated by dividing monocyte numbers migrated in response to PBS. To investigate whether CCL2 contributed to monocyte migration, blocking experiments were performed by mixing the supernatants with 2 μg/ml anti-CCL2 mAb (MAB679-100, R&D systems) or mouse IgG irrelevant isotype control, respectively.

Effects of C5a and IL-1β on proliferation, apoptosis, migration, invasion, adhesion, and EMT of lung cancer cells in vitro

Proliferation

A549 cells were incubated in the presence of serum-free medium alone or with 25 ng/ml C5a, 25 ng/ml C5aRA, or their various combinations (serum-free medium alone, with 10 ng/ml IL-1β, 20 ng/ml IL-1RA, or their various combinations). After incubation for 24 h, A549 cells were trypsinized and harvested, then stained intracellular kit for Ki-67 (eBioscience) and tested by flow cytometry. Cell proliferation ability was also measured by the cell counting kit-8 (CCK-8, Dingguo) following the instructions. Cells were seeded into 96-well culture plates (2×10^3 cells/well) in the different treated medium. Twenty-four hours later, 10 μl CCK-8 solution was added to each well and then incubated at 37°C for another 1–2 h. The absorbance at 450 nm (OD450) was recorded using a microplate reader.

Apoptosis

Apoptotic A549 cells were detected by FITC conjugated Annexin V and propidium iodide (Annexin V FITC Apoptosis Detect Kit; 556 547, BD) via flow cytometry. The lysates of A549 were prepared, and Western blot used to detect the apoptosis-associated protein, including cleaved-Caspase3 and Bax.

Migration

A wound scratch assay was used to determine migratory ability. Confluent monolayers of cultured A549 were scratched with the tip of a p-200 pipette. The cells were rinsed three times with PBS and afterwards incubated in the presence of medium alone or C5a, C5aRA, or their combination (IL-1β, IL-1RA, or their combination). Images of the wound scratches were captured each time at 0, 24, 36 and 48 h. The remaining gap between migrating A549 was measured with Image J and expressed as a percentage of the initial scratched area.

Invasion

A transwell chemotaxis assay was used to determine the invasion ability. Approximately 5×10^4 cells in serum-free medium were seeded into the 24-well Matrigel matrix-coated (Corning) upper chambers, and 500 μl 10% FBS medium with different treatments (C5a, C5aRA, or their combination; IL-1β, IL-1RA, or their combination) were placed in the lower chambers. Over a time period of 24 h, non-invaded cells were wiped off by applying a cotton swab, whereas cells invaded into the lower chambers were fixed and stained using 0.1% crystal violet. Five fields were chosen at random for statistical analysis.

Adhesion

A549 cells were cultured in the presence of serum-free medium alone, C5a, C5aRA, or C5a + C5aRA (IL-1β, IL-1RA, or IL-1β+IL-1RA). After 24 h, the expression of the I-CAM (353 113, Biolegend) in A549 cells was determined by flow cytometry. In the adhesion assay, 10^6 PMCs were seeded in 12-well plates and grown to 90% confluence. Pretreated A549 cells were trypsinized and labeled by CFSE (556547, Biolegend), and then seeded into the washed PMC monolayers for 24 h. Finally, nonadherent A549 cells were removed by washing. Total adherent cells containing A549 cells and PMCs were trypsinized and analyzed by flow cytometry.

Epithelial-to-mesenchymal transition (EMT)

A549 cells were cultured in the presence of serum-free medium alone, C5a, C5aRA, or C5a + C5aRA (IL-1β, IL-1RA, or IL-1β+IL-1RA). After 24 h, A549 cells were trypsinized and harvested, the lysates of A549 were prepared, and Western blot detected the EMT markers, including E-cadherin, N-Cadherin, and Vimentin.

Statistical analysis

Data are expressed as mean ± SD. A Student's *t*-test was used for comparisons of two groups. Comparisons of the data between different groups were performed using one-way ANOVA or Kruskal-Wallis one-way ANOVA. All statistical analyses were performed using GraphPad Prism 10.0 software.

RESULTS

Proportion of $CD14^{++}CD16^{+}$ intermediate monocytes were significantly increased in malignant pleurisy patients

The distribution of monocytes and lymphocytes in routine blood tests of MPE patients and healthy subjects was first investigated. There was a significant increase in the number and proportion of monocytes in MPE patients compared with those in healthy subjects, while the proportion of lymphocytes tended to decrease in the blood of malignant pleurisy patients (Figure 1(a)).

By flow cytometry, we determined that the proportion of monocytes in MPE samples was increased in comparison with the corresponding blood samples (Figure 1(b)). Furthermore, a significantly elevated proportion of monocytes was found in the pleural effusion of MPE patients compared with patients with transudate pleural effusion (Figure 1(b)).

To further identify the phenotypic characteristics of the accumulating monocytes in MPE, CD14 and CD16 were used as classify markers. Our flow cytometry data indicated that the proportions of $CD14^{++}CD16^{+}$ intermediate monocytes were significantly increased in the blood and pleural effusion of the MPE group compared to the transudate group. In contrast, the proportion of the classical $CD14^{++}CD16^{-}$ monocyte subtype was decreased in the blood and pleural effusion of MPE patients. Furthermore, the proportion of the $CD14^{++}CD16^{+}$ subset in MPE was 12 times higher than that of the corresponding peripheral blood compartments (Figure 1(c),(d)). Our results indicated that non-classical monocytes were enriched, prompting us to explore the mechanism of intermediate monocyte migration to the pleural space and its function in MPE.

The classical and alternative pathways of complement activation in MPE patients

We then sought to investigate activation of the complement system in the pathogenesis of MPE. By immunohistochemistry, we detected the presence of motive factors of the classical (C1q) and alternative pathways (factor B), while little presence of the mannose-binding lectin (MBL) pathway was observed (Figure 2(a)). Expression of the regulatory components of the alternative pathway (factor P) was observed in MPE, but no expression of the deactivator of the alternative pathway (factor H) was detected. Unexpectedly, we detected no C3a expression but high expression of C5a in malignant pleurisy tissues. Moreover, expression of the terminal product of the complement membrane attack complex (SC5b-9) was significantly increased in malignant pleurisy (Figure 2

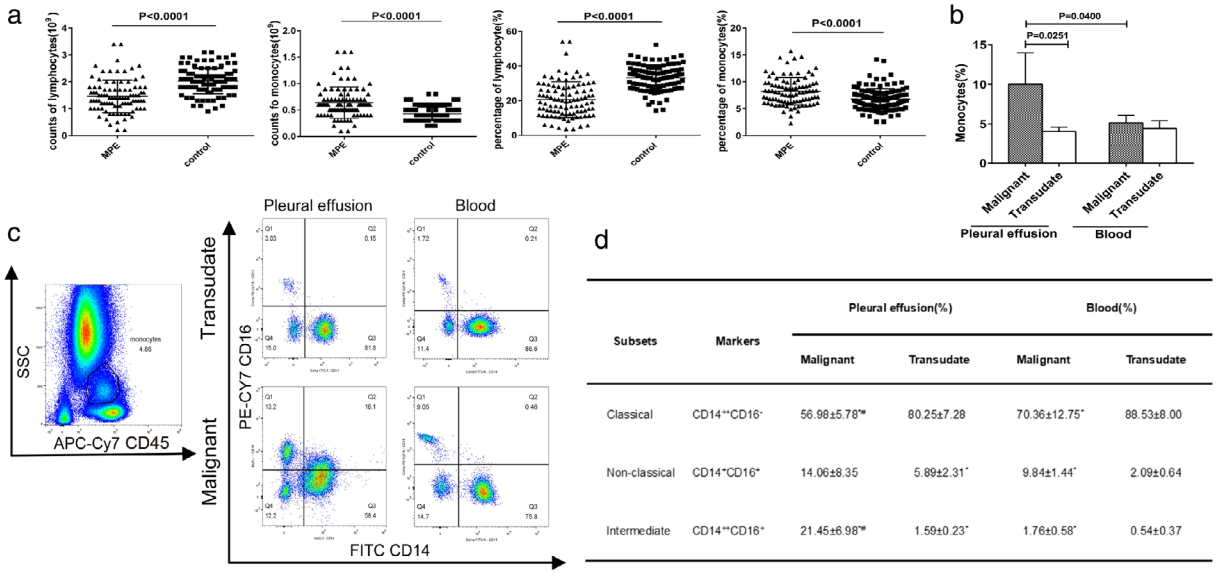

Subsets	Markers	Pleural effusion(%)		Blood(%)	
		Malignant	Transudate	Malignant	Transudate
Classical	$CD14^{++}CD16^{-}$	56.98±5.78*#	80.25±7.28	70.36±12.75*	88.53±8.00
Non-classical	$CD14^{+}CD16^{+}$	14.06±8.35	5.89±2.31*	9.84±1.44*	2.09±0.64
Intermediate	$CD14^{++}CD16^{+}$	21.45±6.98*#	1.59±0.23*	1.76±0.58*	0.54±0.37

FIGURE 1 Increased $CD14^{++}$ $CD16^{+}$ intermediate monocytes in MPE patients (a) absolute counts and percentages of total monocytes and lymphocytes in blood samples from MPE patients and healthy subjects. ($n_{malignant} = 94$, $n_{healty} = 102$). (b) Flow cytometry analysis of percentages of total monocytes in pleural effusion and blood from MPE patients ($n_{malignant} = 10$, $n_{transudate} = 10$). (c) Representative flow cytometry dot plots showing monocyte subsets in patients with malignant and transudate pleural effusion. Monocytes were first identified within SSC-A^{hi} FSC-A^{hi} cells and subsequently gated for either $CD14^{++}CD16^{-}$, $CD14^{++}CD16^{+}$ or $CD14^{+}CD16^{+}$ subsets. (d) Summary data of monocytes subsets in pleural effusion and blood samples ($n_{MPE} = 10$, $n_{transudate} = 6$). *Vs. transudate pleural effusion and blood. *$p < 0.05$. #Vs corresponding blood, #$p < 0.05$

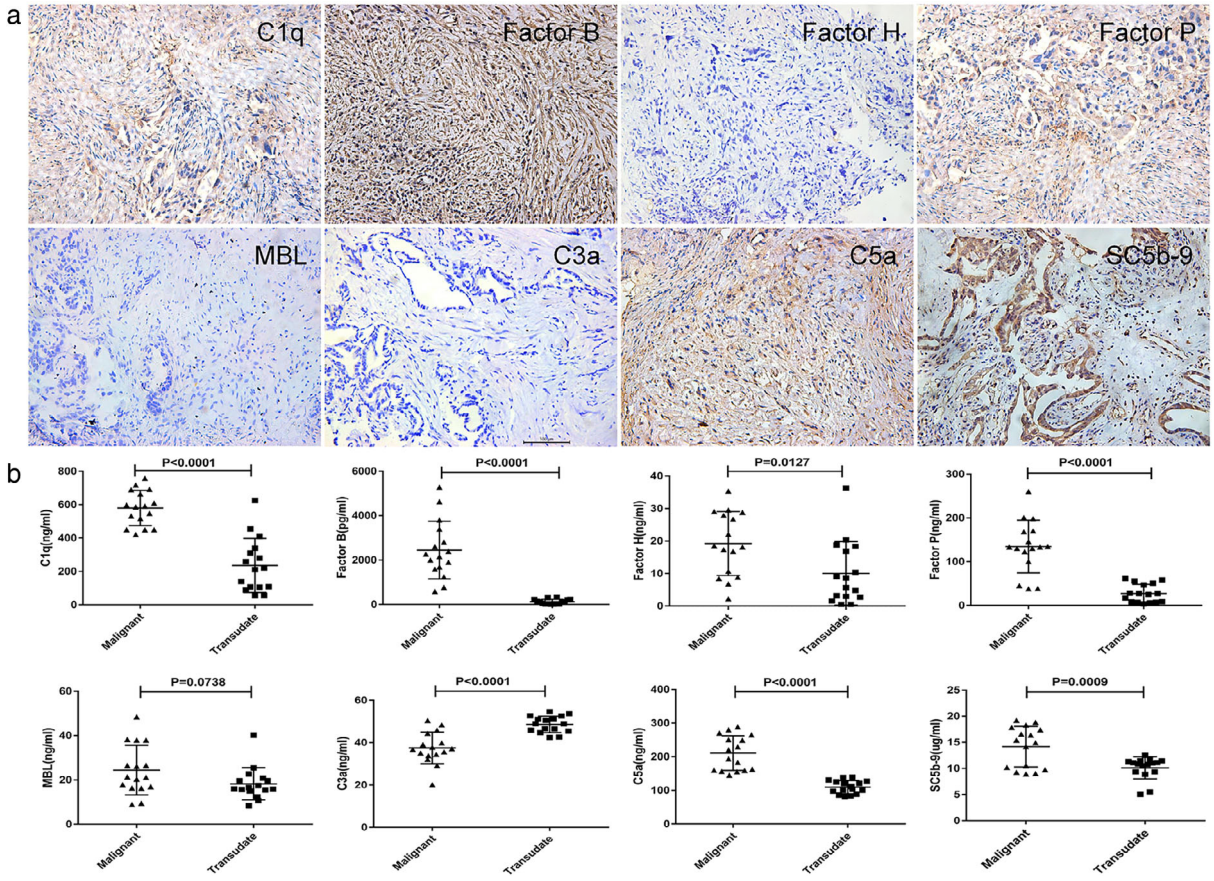

FIGURE 2 Complement system classical and alternative pathways were activated in patients with malignant pleurisy. (a) Representative immunohistochemistry staining images of pleurisy tissues from MPE patients. Three complement pathway components, including C1q, factor B, MBL, factor H, factor P, C3a, C5a, and SC5b-9 (original magnification,×200) were detected. (b) The concentrations of complement components from pleural effusion were measured by ELISA ($n_{MPE} = 16$, $n_{transudate} = 16$)

(a)). In summary, our immunohistochemistry data demonstrated that, classical and alternative pathways were activated in MPE, leading to high expression of C5a, while MBL, factor H and C3a were not expressed.

By using ELISA, we further confirmed that the levels of complement components (C1q, factor B, factor P, Factor H, C5a, and SC5b-9) were higher in the MPE group than the transudate group. At the same time, the C3a level was decreased in MPE, which was consistent with the immunohistochemistry results (Figure 2(b)). Considering the absence of C3a expression and elevated C5a level in MPE, we further studied the effect of C5a on intermediate monocytes in the MPE environment.

C5a enhances recruitment of $CD14^{++}CD16^{+}$ intermediate monocytes via the CCL2-CCR2 axis by PMCs

We sought to explore the role of chemokines induced by C5a in the infiltration of intermediate monocytes in MPE. First, our results showed that the concentration of CCL2, but not CCL7 or CX3CL1, was much higher in MPE than transudate pleural effusion (Figure 3(a)). Then, using immunofluorescence staining, we demonstrated CCL2-CCR2 and C5a-C5aR coexpression in PMCs and intermediate monocytes from MPE (Figure 3(b)). A similar result was obtained by real-time PCR, which showed that the expression levels of CCL2 and CCR2 in intermediate monocytes were significantly elevated in the MPE group compared to the transudate group, and PMCs in the MPE group expressed higher CCL2 than those in the transudate group (Figure 3(c)). Moreover, C5a could significantly stimulate CCL2 expression in PMCs (Figure 3(d),(e)). The transwell assay results further indicated that PMC culture supernatant exerted a potent chemoattractant effect on $CD14^{++}CD16^{+}$ monocytes, whereas anti-CCL2 mAbs significantly suppressed monocyte chemotaxis (Figure 3(f)), suggesting that the chemotaxis of intermediate monocytes promoted by PMCs was mediated by the C5a-induced CCL2-CCR2 axis.

C5a enhances IL-1β release from $CD14^{++}CD16^{+}$ intermediate monocytes in MPE

As shown in Figure 4(a), the concentrations of IL-1β and IFN-γ in the supernatant were significantly increased in the

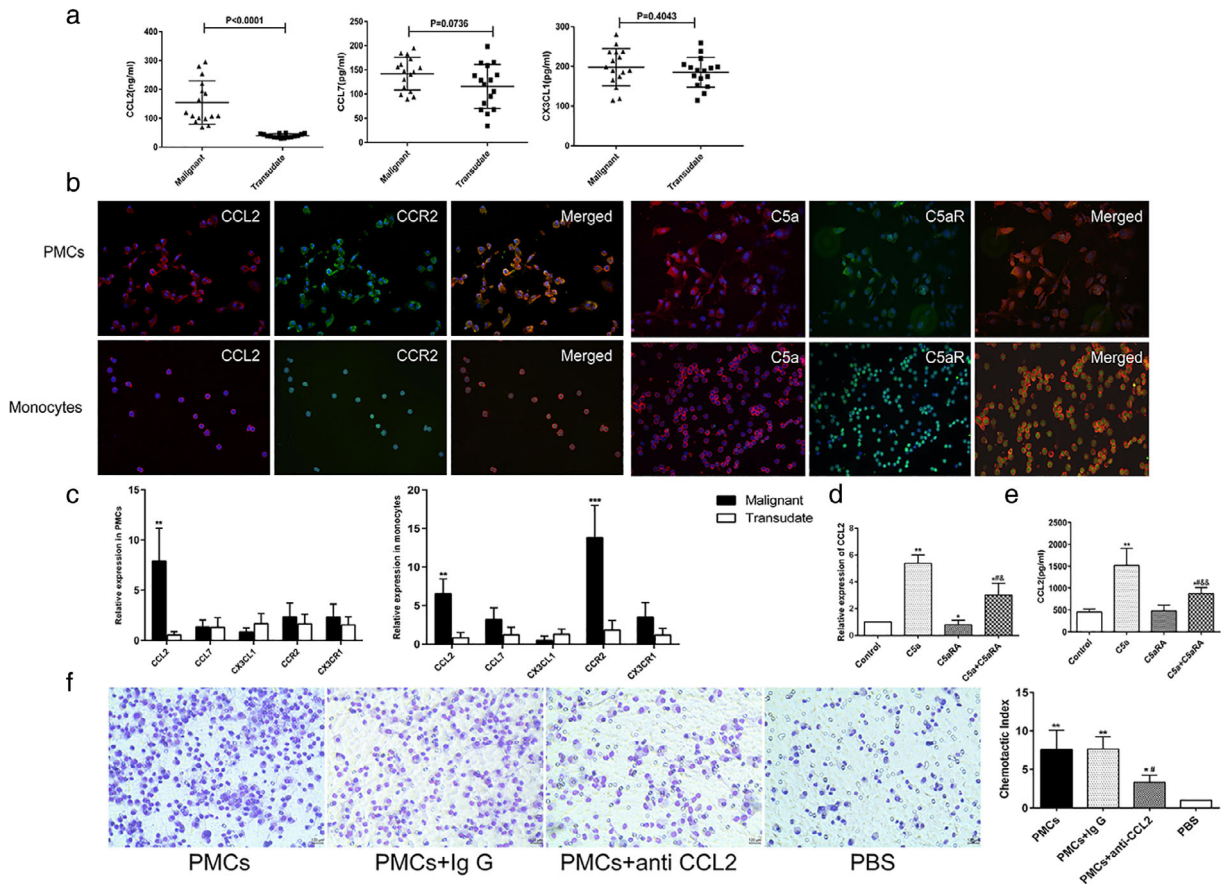

FIGURE 3 C5a enhanced the recruitment of $CD14^{++}CD16^{+}$ intermediate monocytes through CCL2/CCR2 axis in MPE. (a) Expression levels of chemokines CCL2, CCL7, and CX3CL1 in pleural effusion were measured by ELISA ($n_{MPE} = 16$, $n_{transudate} = 16$). (b) Representative immunofluorescence images of CCL2-CCR2 and C5a-C5aR coexpression in PMCs and $CD14^{++}CD16^{+}$ monocytes from malignant pleural effusion (×200). (c) Real-time qPCR analysis of chemokines and their receptors expression in $CD14^{++}CD16^{+}$ monocytes ($n_{MPE} = 10$, $n_{transudate} = 6$) and PMCs ($n_{MPE} = 5$, $n_{transudate} = 5$) from pleural effusion. The expression levels of target genes were normalized to housekeeping gene GAPDH. *Versus. transudate group, $^{**}p < 0.01$, $^{***}p < 0.0001$. (d) The expression of CCL2 in PMCs after treatment with either C5a, C5aRA, or C5a and C5aRA was analyzed by real-time qPCR ($n = 3$). *Versus control group, $^{**}p < 0.01$.$^{\#}$Versus C5a group, $^{\#}p < 0.05$. $^{\&}$Versus C5aRA group, $^{\&}p < 0.05$, $^{\&\&}p < 0.01$. (e) The concentration of CCL2 in PMCs after treatment with either C5a, C5aRA, or C5a and C5aRA was analyzed by ELISA ($n = 3$). *Versus control. $^{**}p < 0.01$. $^{\#}$Versus C5a group, $^{\#\#}p < 0.01$. $^{\&}$Versus C5aRA group, $^{\&}p < 0.05$. (f) Representative chemotaxis images of $CD14^{++}CD16^{+}$ monocytes cultured in supernatants from PMCs. The supernatants were added with either isotype IgG, anti-CCL2, or PBS in the bottom chamber of transwells (×200). *Versus PBS group, $^{*}p < 0.05$, $^{**}p < 0.01$. $^{\#}$Versus PMCs group. $^{\#}p < 0.05$

MPE group compared to the transudate group (Figure 4(a)), while there was no significant difference in IL-27 and IL-17 expression. Consistent with the supernatant results, the mRNA level of IL-1β in $CD14^{++}$ $CD16^{+}$ intermediate monocytes isolated from MPE patients was also significantly higher than that in transudate subjects, whereas IL-17 and IL-27 were lower in the MPE group (Figure 4(b)). Unexpectedly, the transcription of IFN-γ in intermediate monocytes from MPE was downregulated, which showed a different trend from the ELISA result of pleural effusion supernatant (Figure 4(b)). Next, after C5a stimulation, the IL-1β expression in the presence of LPS in intermediate monocytes were increased elevated, while C5aRA could prevent this stimulation (Figure 4(c)). As shown in Figure 4(d), ELISA detection of monocyte culture supernatant showed a similar result. Our findings indicated that C5a enhanced IL-1β release from $CD14^{++}CD16^{+}$ intermediate monocytes in MPE

C5a plays a role in the proliferation, apoptosis, migration, invasion, adhesion, and EMT of lung cancer cells

To investigate the role of C5a in the progression of MPE, we first evaluated the effects of C5a on the proliferation of A549 cells. As indicated by Ki-67 expression levels and the CCK-8 assay, C5a subsantially promoted A549 cell proliferation, while C5aRA suppressed it (Figure 5(a),(b)). By western blot, we further found that C5a caused a significant increase in the levels of p-AKT and PI3K expression, and this effect could be inhibited by C5aRA (Figure 5(c)). The PI3K inhibitor LY29f4002 resulted in a decrease in Ki-67-positive A549 cells and a lower proliferation index than C5a treatment alone (Figure 5(d),(e)).

As flow cytometry and Western blot results indicated, neither C5a nor C5aRA exerted a significant effect on the

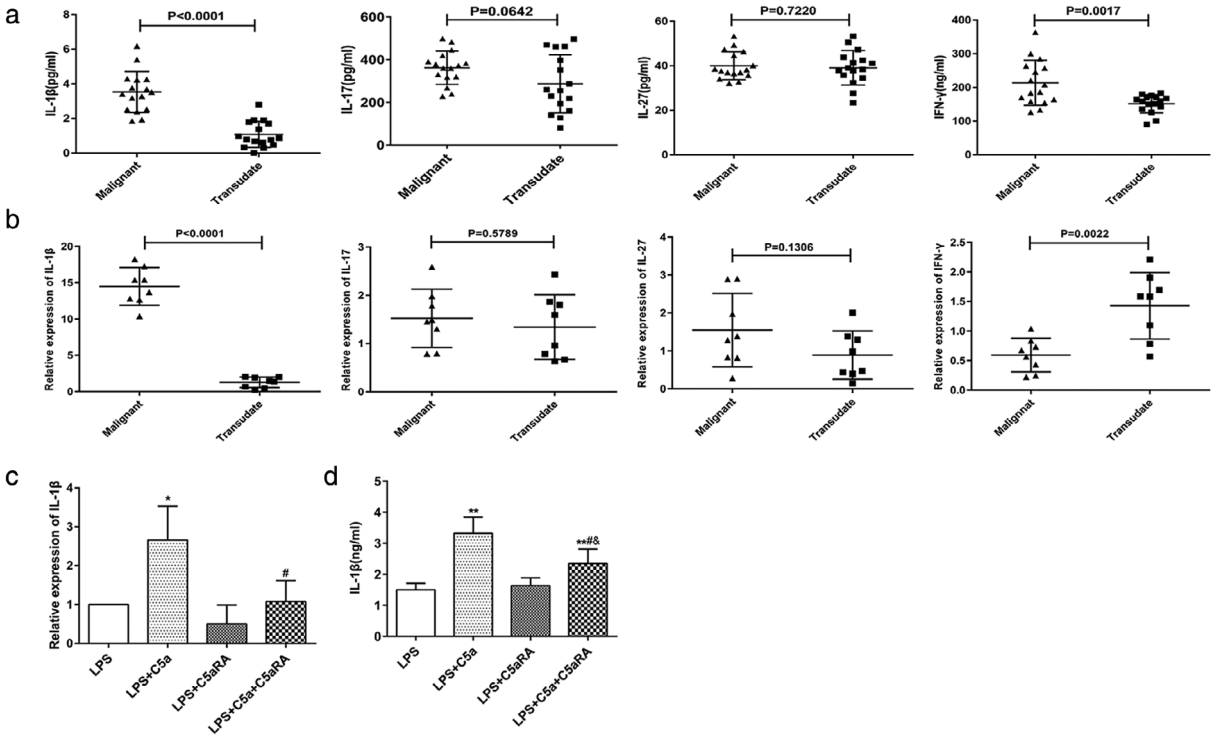

FIGURE 4 C5a–C5aR axis promoted IL-1β production in $CD14^{++}CD16^{+}$ intermediate monocytes. (a) The concentrations of inflammatory cytokines (IL-1β, IL-17, IL-27, and IFN-γ) in pleural effusion were measured by ELISA ($n_{MPE} = 16$; $n_{transudate} = 16$). (b) The expression levels of inflammatory cytokines (IL-1β, IL-17, IL-27, and IFN-γ) in intermediate monocytes were measured by qRT-PCR ($n_{MPE} = 16$; $n_{transudate} = 16$). (c) The expression levels of IL-1β in $CD14^{++}CD16^{+}$ intermediate monocytes after either C5a or C5aRA treatment ($n = 3$) in the presence of LPS were measured by qRT-PCR. *Versus control group, $^{*}p < 0.05$. #Versus C5a group, $^{\#}p < 0.05$. (d) The expression levels of IL-1β in $CD14^{++}CD16^{+}$ intermediate monocytes after either C5a or C5aRA treatment ($n = 3$) in the presence of LPS were measured by ELISA ($n = 3$). *Versus control. $^{**}p < 0.01$. #Versus C5a group, $^{\#}p < 0.05$. &Versus C5aRA group, $^{\&}p < 0.05$

apoptosis of A549 cells (Figure 5(f),(g)). Cisplatin (DDP) is an effective drug that induces apoptosis in cancer cells, possibly via caspase-3 activation. To determine whether C5a exerts an effect on DDP-induced apoptosis in tumor cells, A549 cells were treated with C5a or C5aRa in the presence of DDP. As shown in Figure 5(h),(i), the apoptosis of A549 cells and the protein levels of cleaved-Caspase 3 and Bax were significantly decreased in the C5a + DDP group, while they were elevated in the C5aRA + DDP group, and C5a could reverse the increase in apoptosis caused by C5aRA.

We then sought to investigate whether C5a was involved in the regulation of tumor cell migration and invasion. As soon as 24 h after wounding, C5a showed promoting effects on A549 wound closure (Figure 5(j)). Unexpectedly, incubation with C5aRA alone had no effects on A549 migration, while it was harmful to C5a-enhanced A549 cell wound healing (Figure 5(j)). As expected, the addition of C5a strongly promoted tumor invasion activity. Although the addition of C5aRA alone did not affect this invasion activity, it significantly suppressed the invasion activity increased by C5a (Figure 5(k)).

The expression of intercellular adhesion molecule-1 (ICAM-1, CD54) was significantly elevated after C5a treatment, which could be abolished by the addition of C5aRA (Figure 5(l)). An adhesion assay further confirmed that a significant number of A549 cells adhered to the PMC monolayer within 24 h. As expected, C5a strongly enhanced adhesion, while C5aRA abrogated the enhanced adhesion activity of tumor cells and PMCs (Figure 5(m)). Moreover, Western blot results demonstrated that the levels of N-cadherin and vimentin, markers of mesenchymal cells, were significantly increased in C5a-treated A549 cells, whereas the expression of E-cadherin, an epithelial cell marker, was severely decreased. Our results also indicated that C5aRA had the opposite effect on EMT in A549 cells as C5a (Figure 5(n)).

IL-1β plays a role in the proliferation, apoptosis, migration, invasion, adhesion, and EMT of lung cancer cells

As shown in Figure 6(a),(b), Ki-67 expression and the proliferation index of A549 cells were increased in the presence of IL-1β, and this effect was dramatically inhibited by the IL-1R antagonist (IL-1RA). The MAPK pathway is the best-known signaling pathway in the development of cancer and regulates important cellular processes such as proliferation. We then assessed the protein levels of MAPK and p-MAPK in treated A549 cells and found that IL-1β treatment resulted in a significant increase in the levels of MAPK and

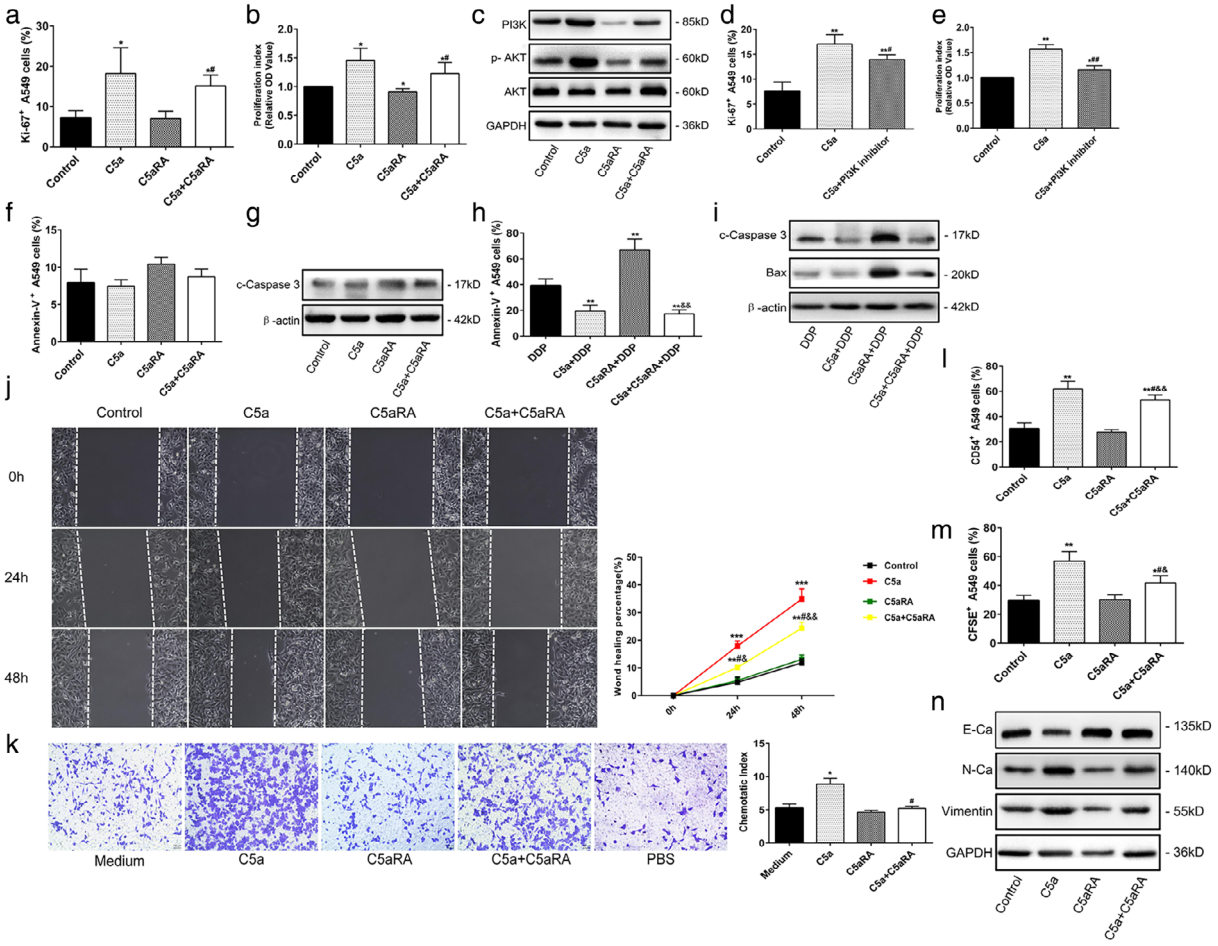

FIGURE 5 Role of C5a in the proliferation, apoptosis, migration, invasion, adhesion, and EMT of A549 cells. (a) Ki-67$^+$ expression was measured by flow cytometry ($n = 3$) after treatment with either recombinant human C5a, C5aR antagonist (50 nM), or C5a and C5aR. (b) The proliferation index of A549 cells calculated by CCK8 ($n = 3$). (c) PI3K, p-PI3K, and AKT expression was detected by Western blot. (d) Ki-67$^+$ expression was determined by flow cytometry ($n = 3$) after treatment with or without PI3K inhibitor in the presence of C5a. (e) The proliferation index of A549 cells in the presence of PI3K inhibitor ($n = 3$). (f) The percentages of apoptotic A549 cells were analyzed by Annexin-V$^+$ staining in flow cytometry ($n = 3$). (g) The expression levels of cleaved-caspase 3 were analyzed by Western blot. (h) Ki-67$^+$ expression was measured in the presence of DDP by flow cytometry ($n = 3$). (i) The protein levels of cleaved-caspase 3 and Bax were detected by Western blot. (j) Microscopic photography of A549 cells after wound induction at 24 and 48 h (×200). Wound healing percentage = (Area$_{0h}$ − Area$_{xh}$)/ Area$_{0h}$ × 100%. (k) The chemotaxis of A549 (×200) ($n = 3$). l) CD54 (I-CAM) expression was determined by flow cytometry ($n = 3$). (m) Flow cytometry analysis of CFSE$^+$ cells in the adhesion assay. (n) The protein levels of E-cadherin, N-cadherin, and vimentin were detected by Western blot ($n = 3$). *Versus. control group, $^*p < 0.05$, $^{**}p < 0.01$, $^{***}p < 0.001$. $^{\#}$Versus C5a group, $^{\#}p < 0.05$, $^{\#\#}p < 0.01$. $^{\&}$Versus C5aRA group, $^{\&}p < 0.05$, $^{\&\&}p < 0.01$

p-MAPK, while IL-1RA significantly prevented the activation of MAPK signaling (Figure 6(c)). Our data showed that apoptosis was significantly lower in IL-1β-treated cells than in untreated control cells, while the IL-1β receptor antagonist significantly stimulated the apoptosis of A549 cells (Figure 6(d),(e)).

As the wound-healing assay showed, there was a significant decline in A549 migration in the IL-1RA group compared to the control group after 36 h (Figure 6(f)). As the transwell assay showed, in the presence of IL-1β, tumor invasion activity was promoted, while the addition of IL-1RA significantly prevented the increase in invasion capability caused by IL-1β (Figure 6(g)).

In addition, IL-1β significantly induced ICAM-1 expression in lung cancer cells, and this effect was abolished by the addition of IL-1RA (Figure 6(h)). As shown in Figure 6(i), IL-1β strongly enhanced the adhesion of A549 cells to the PMC monolayer, while IL-1RA abrogated the adhesion capability. As indicated in the Western blot results in Figure 6(j), IL-1β increased the expression of N-cadherin and vimentin, whereas it had no effect on E-cadherin. IL-1RA had the opposite effect on EMT markers compared with IL-1β.

DISCUSSION

In previous studies, we reported that the anaphylatoxins C3a and C5a could enhance the homing of nonclassical monocytes to the pleural cavity by the chemokine axis in

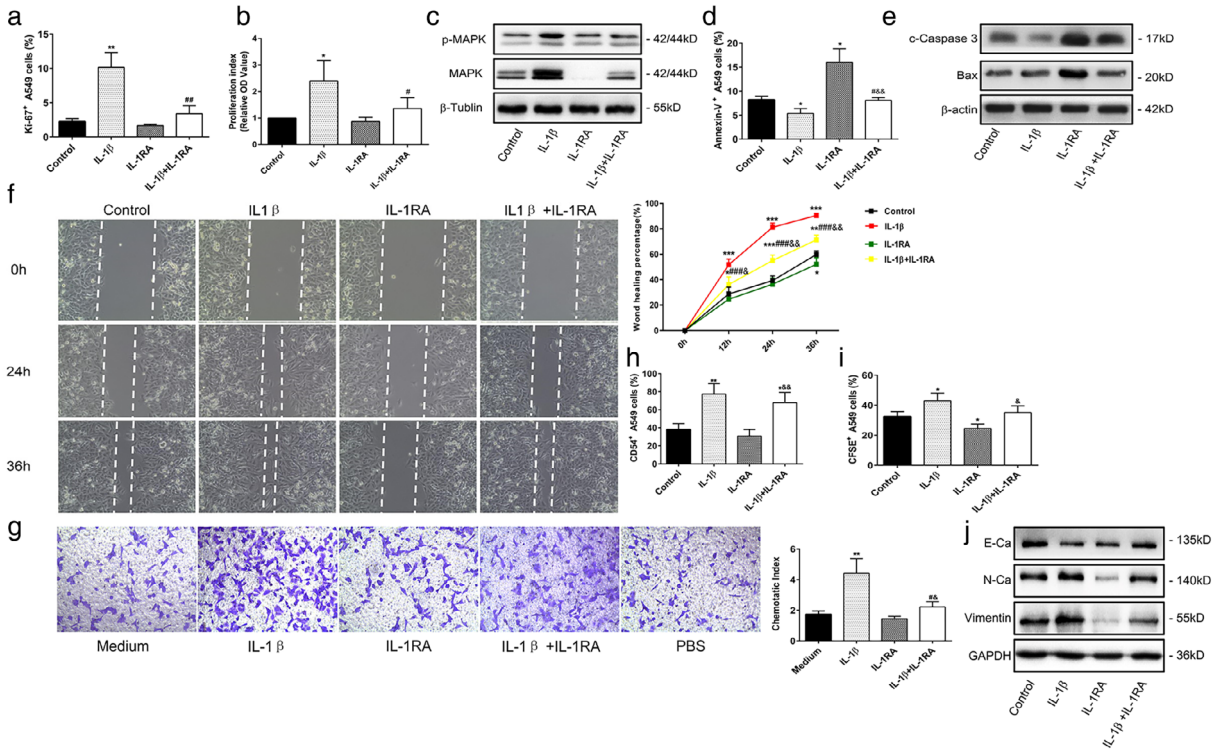

FIGURE 6 Role of IL-1β in the proliferation, apoptosis, migration, invasion, adhesion, and EMT of A549 cells. (a) Ki-67$^+$ A549 cells were determined by flow cytometry ($n = 3$) after treatment with recombinant human IL-1β (10 ng/ml), IL-1R antagonist (20 ng/ml) or their combination. (b) The proliferation index of A549 cells calculated by CCK8 ($n = 3$). (c) The protein levels of MAPK and p-MAPK were observed by Western blot. (d) Apoptotic A549 cells were determined by Annexin-V$^+$ A549 cells ($n = 3$). (e) The protein levels of cleaved-caspase 3 and Bax were observed by Western blot after treatment. (f) Microscopic photography of A549 cells after wound induction for 24 and 36 h (×200) ($n = 3$). (g) The chemotaxis of A549 cells (×200) ($n = 3$). (h) The CD54 (I-CAM) expression of A549 was determined by flow cytometry ($n = 3$). (i) The CFSE$^+$ percentage of total cocultured A549 and PMCs cells were assayed by flow cytometry ($n = 3$). (j) The protein levels of E-cadherin, N-cadherin, and vimentin were observed by Western blot after treatment. *Versus control group, $^*p < 0.05$, $^{**}p < 0.01$, $^{***}p < 0.001$. $^{\#}$Versus IL-1β group, $^{\#}p < 0.05$, $^{\#\#}p < 0.01$, $^{\#\#\#}p < 0.001$. $^{\&}$Versus IL-1RA group, $^{\&}p < 0.05$, $^{\&\&}p < 0.01$

tuberculosis pleural effusion (TPE).[21] In the present study, we extended our previous work and demonstrated that the activation of C5a in MPE induced the recruitment of intermediate monocytes and played an essential role in the progression of MPE.

In the context of cancer, complement C3a and C5a, which leads to tumor-promoting chronic inflammation in the majority of the studied mouse models, are continually generated.[23] However, the molecular mechanisms underlying the activation of the complement system, especially C3a and C5a, in MPE remain unknown. In the present study, we observed activation of the classical and alternative pathways, while little presence of the MBL pathway in malignant pleurisy tissue (Figure 2), which is different from tuberculous pleurisy.[21] Li et al. elucidated an unknown feature of MBL function in suppressing tumor development.[24] Consistent with their results, we also detected no MBL expression in MPE, indicating that in advanced tumors, low or even no MBL expression is favorable to tumor development and promotes tumor growth. Considering the differential activation of the complement pathway in MPE and TPE, the expressions of complement factors in pleural effusion might be a promising diagnostic marker. In the present study, we detected high activation of C5a and low levels of C3a, both by immunohistochemistry and ELISA. Our data were consistent with those reported by Bulla and colleagues,[15] which revealed a strong signal for C1q in lung adenocarcinoma and mild expression of C3. Thus, the activation of the classical and alternative pathways is increased in MPE and may be responsible for the high level of C5a. Because C5a is a strong chemoattractant for inflammatory cells, the major focus of this study was to explore the role of C5a and monocytes in MPE progression.

Emerging evidence indicates that monocytes contribute to carcinogenesis by releasing inflammatory mediators.[25] Wang et al. reported that the CD163$^+$CD14$^+$ and CD206$^+$CD14$^+$ cell frequencies in MPE were markedly higher than those in benign pleural effusion, and these CD14 positive cells could potentially be used as an immune diagnostic marker for MPE.[26,27] However, the authors did not analyze the subtype of monocytes in MPE. In agreement with Wang et al. our data also revealed that the portion of monocytes was higher in MPE, showing significant increases compared to those in the blood (Figure 1(a),(b)). In addition, we demonstrated that CD14^{++}CD16$^-$ classical monocytes were decreased in malignant pleurisy patients, while

$CD14^{+}CD16^{+}$ nonclassical and $CD14^{++}CD16^{+}$ intermediate monocytes were significantly increased in MPE, which was different from the observations in TPE.[21] Interestingly, the proportion of $CD14^{++}CD16^{+}$ monocytes in MPE was 12 times higher than that in peripheral blood (Figure 1(c),(d)). However, it is unclear how these accumulating intermediate monocytes enter the pleural cavity and whether they promote the progression of MPE.

Monocytes were found to be recruited by complement C5a through the increased secretion of chemokines, including CCL2, in severe COVID-19 patients.[28] Our previous results also demonstrated that C5a mediated the infiltration of monocytes into the pleural cavity by inducing the expression of chemokines (CCL2, CCL7 and CX3CL1) released by PMCs in TPE.[21] These studies indicated that C5a was a strong chemoattractant for monocytes. In lung cancer, Ajona et al. reported that blockade of the C5a-C5aR1 axis resulted in a substantial improvement in the efficacy of anti-PD-1 antibodies against lung cancer growth and metastasis through CXCL16-mediated effects.[29] We demonstrated high expression of CCL2 but no difference in CCL7 or CX3CL1 expression in MPE compared with transudate plural effusion (Figure 3(a),(b)). Additionally, intermediate monocytes and PMCs in MPE expressed high levels of CCL2 but low levels of CCL7 and CX3CL1 (Figure 3(c)). Our results demonstrated that intermediate but not nonclassical monocytes play an important role in MPE. C5a significantly enhanced the secretion of CCL2 from PMCs (Figure 3(d),(e)). Considering our present results showing the enrichment of intermediate monocytes in MPE compared to the corresponding peripheral blood, as well as the high activation of C5a, we hypothesized that intermediate monocytes could leave the bloodstream and home to pleural effusion through C5a-inducing chemokines in MPE. To test this hypothesis, we performed an in vitro transwell assay to elucidate the mechanism underlying intermediate monocyte accumulation in MPE. The results showed that C5a-treated PMCs promoted the migration of intermediate monocytes, while the anti-CCL2 mAb significantly inhibited the ability of supernatants to stimulate monocyte chemotaxis (Figure 3(f)). Therefore, PMC-produced CCL2 might act as a chemoattractant of intermediate monocytes into the pleural cavity in MPE, and C5a could facilitate the CCL2-CCR2 pathway.

Compared with other monocyte subsets, intermediate monocytes in humans express higher levels of proinflammatory cytokines, such as IL-1β,[30,31] which promotes the progression of tumors.[32] However, the role of cytokines released by intermediate monocytes in MPE needs to be further elucidated. Our data showed a significant increase in IL-1β expression in MPE supernatant and a higher level of IL-1β secretion in intermediate monocytes isolated from MPE (Figure 4(a),(b)). Consistent with a previous in vitro study in neutrophils,[33] our data showed that C5a has the potential to induce the generation of LPS-stimulated IL-1β in intermediate monocytes (Figure 4(c),(d)). Collectively, our results demonstrated that the C5a-C5aR axis not only regulates the infiltration of intermediate monocytes into the pleural cavity, but also increases the proportion of IL-1β-releasing intermediate monocytes, which participate in the immune response in MPE.

Although C5a has been reported to be an essential mediator of inflammation-induced tumorigenesis, little information is known about its role in the progression of tumor cells.[17] We found that C5a induced A549 cell proliferation in lung cancer, which was consistent with the findings of Chen et al.[20] Chen et al. also proved that the C5a-C5aR pathway participates in the pathogenesis of gastric cancer via activation of the PI3K/AKT axis.[19] Similarly, our results showed that C5a treatment led to a highly significant increase in the levels of p-AKT. Furthermore, the PI3K inhibitor LY29f4002 was reported to inhibit A549 proliferation in the presence of C5a (Figure 5(d),(e)). Thus, it is plausible to suggest that C5a-C5aR signaling regulates the proliferation of lung carcinoma cells via PI3K/AKT axis activation. Some reports have indicated that the C5a-C5aR axis decreases apoptosis in several cell types, such as neutrophils,[34] T cells,[35] and macrophages.[36] Our current study suggested that the C5a–C5aR axis could protect lung cancer cells from DDP-induced apoptosis (Figure 5(h),(i)). The migration, invasion, adhesion, and EMT of tumor cells are also important factors influencing tumor metastasis. Our data revealed that C5a facilitated the migration and invasion of lung carcinoma cells (Figure 5(j),(k)). Additionally, C5a was reported to promote the intercellular adhesion of A549 cells to PMCs (Figure 5(l),(m)), consistent with previous studies, which proved that C5a was the principal initiator of neutrophil adhesion by regulating cell adhesion molecules.[37] Furthermore, the C5a axis showed a similar role in promoting EMT in A549 cells (Figure 5(n)) as it did in renal tubular epithelial cells.[38] Overall, our study revealed that C5a exerted a tumor-promoting effect by inducing the proliferation, migration, invasion, adhesion, and EMT of A549 cells and inhibiting the apoptosis of tumor cells, while C5aRA significantly reversed these effects.

IL-1β has emerged as a key component of tumor-promoting inflammation by shaping different elements of the tumor microenvironment, including cancer cell proliferation,[32,39] migration, and metastasis.[32,40] Based on our data showing that C5a has the ability to induce IL-1β secretion from intermediate monocytes, we attempted to explore the role of IL-1β overexpression stimulated by C5a. Here, we demonstrated that the IL-1β/IL-1R axis could promote the proliferation of A549 cells in vitro (Figure 6(a),(b)), which was consistent with previous studies on human natural killer cells and glioblastoma cells.[41] We also found a tendency towards the upregulation of MAPK/p-MAPK expression in A549 cells after IL-1β treatment (Figure 6(c)), but further study is needed to confirm whether the MAPK signaling pathway is the main mechanism by which IL-1β induces the growth of tumor cells. According to previous studies, the IL-1β/IL-1R axis is also a regulator of apoptosis in several cell types.[42] Our study reached a similar conclusion, showing that the IL-1β/IL-1R axis regulates the apoptosis of A549 cells (Figure 6(d),(e)). Although IL-1β is responsible for migration/invasion and has been shown to

be produced by cells in the tumor microenvironment, such as macrophages, fibroblasts, and B-cells,[33] the mechanism by which IL-1β induces the formation of MPE by shaping the metastasis of tumor cells in the pleural cavity is poorly understood. As shown in Figure 6(f)–(i), IL-1β promoted cancer cell migration, invasion and adhesion. Moreover, our data in Figure 6(j) showed that the IL-1β/IL-1R axis may have a regulatory role in the EMT of A549 cells, which exerts a similar effect on colon cancer cells.[43] In general, our data showed that IL-1β facilitated the proliferation, migration, invasion, adhesion, and EMT of A549 cells, attenuated the apoptosis of tumor cells, and provided clues for the combination of chemotherapy and IL-1β blockade to improve the outcomes of patients with lung cancer.

In conclusion, our data suggested that the numbers of intermediate monocytes in MPE were significantly increased compared with their compartments in blood and that overrepresentation of intermediate monocytes in MPE may be due to the PMC-produced CCL2 promoted by C5a. Our data also revealed the activation of the classical and alternative pathways of complement in MPE and the initial role of C5a in MPE. Therefore, the estimations of monocyte subsets and complement components might be novel candidate markers for distinguishing different pleural effusions. Further investigation showed that the C5a–C5aR axis between pleural mesothelial cells and intermediate monocytes in MPE was responsible for the overexpression of IL-1β by intermediate monocytes, which could represent an immunological pathogenic mechanism of malignant pleural effusion. Hence, blocking C5a–C5aR axis by antagonists alleviated the IL-1β inflammatory in monocytes, further reducing the formation of malignant pleural effusion. Moreover, C5a and IL-1β significantly increased the proliferation, migration, invasion, adhesion, and EMT of tumor cells and inhibited apoptosis in vitro. These data add to the emerging role of complement components activated by intermediate monocytes in lung tumor progression and metastasis and raise the possibility that C5a contributes to a tumor-associated microenvironment that fosters tumor cell aggressiveness.

ACKNOWLEDGMENTS

We thank Dr Hongmei Chen and Bingrong Zhao for specimen collection. This study was supported by the Natural Science Foundation of Hunan Province (2020JJ4887), the Key Research and Development Program of Hunan Province (2021SK2033), clinical medical technology innovation guidance program of Hunan Province (2020SK53701).

CONFLICT OF INTEREST

All authors: No potential conflicts of interest. All authors have submitted the ICMJE Form for Disclosure of Potential Conflicts of Interest. Conflicts that the editors consider relevant to the content of the manuscript have been disclosed.

ORCID

Juntao Feng https://orcid.org/0000-0002-2674-9744

REFERENCES

1. Walker S, Mercer R, Maskell N, Rahman NM. Malignant pleural effusion management: keeping the flood gates shut. Lancet Respir Med. 2019;8:609–18. https://doi.org/10.1016/S2213-2600(19)30373-X
2. Light RW. Pleural effusions. Med Clin North Am. 2011;95:1055–70. https://doi.org/10.1016/j.mcna.2011.08.005
3. Ye ZJ, Zhou Q, Yin W, Yuan ML, Yang WB, Xiong XZ, et al. Differentiation and immune regulation of IL-9-producing CD4+ T cells in malignant pleural effusion. Am J Respir Crit Care Med. 2012;186:1168–79. https://doi.org/10.1164/rccm.201207-1307OC
4. Ye ZJ, Zhou Q, Zhang JC, Li X, Wu C, Qin SM, et al. CD39+ regulatory T cells suppress generation and differentiation of Th17 cells in human malignant pleural effusion via a LAP-dependent mechanism. Respir Res. 2011;12:77–87. https://doi.org/10.1186/1465-9921-12-77
5. Ye ZJ, Zhou Q, Yin W, Yuan ML, Yang WB, Xiang F, et al. Interleukin 22-producing CD4+ T cells in malignant pleural effusion. Cancer Lett. 2012;326:23–32. https://doi.org/10.1016/j.canlet.2012.07.013
6. Feng PH, Lee KY, Chang YL, Chan YF, Kuo LW, Lin TY, et al. CD14+S100A9+ monocytic myeloid-derived suppressor cells and their clinical relevance in non-small cell lung cancer. Am J Respir Crit Care Med. 2012;186:1025–36. https://doi.org/10.1164/rccm.201204-0636OC
7. Porrello A, Leslie PL, Harrison EB, Gorentla BK, Kattula S, Ghosh SK, et al. Factor XIIIA-expressing inflammatory monocytes promote lung squamous cancer through fibrin cross-linking. Nat Commun. 2018;9:1988. https://doi.org/10.1038/s41467-018-04355-w
8. Shi C, Pamer EG. Monocyte recruitment during infection and inflammation. Nat Rev Immunol. 2011;11:762–74. https://doi.org/10.1038/nri3070
9. Carroll MV, Sim RB. Complement in health and disease. Adv Drug Deliv Rev. 2011;63:965–75. https://doi.org/10.1016/j.addr.2011.06.005
10. Merle NS, Noe R, Halbwachs-Mecarelli L, Fremeaux-Bacchi V, Roumenina LT. Complement system part II: role in immunity. Front Immunol. 2015;6:257. https://doi.org/10.3389/fimmu.2015.00257
11. Mathern DR, Heeger PS. Molecules great and small: the complement system. Clin J Am Soc Nephrol. 2015;10:1636–50. https://doi.org/10.2215/CJN.06230614
12. Afshar-Kharghan V. The role of the complement system in cancer. J Clin Invest. 2017;127:780–9. https://doi.org/10.1172/JCI90962
13. Lin K, He S, He L, Chen J, Cheng X, Zhang G, et al. Complement component 3 is a prognostic factor of non-small cell lung cancer. Mol Med Rep. 2014;10:811–7. https://doi.org/10.3892/mmr.2014.2230
14. Niculescu F, Rus HG, Retegan M, Vlaicu R. Persistent complement activation on tumor cells in breast cancer. Am J Pathol. 1992;140:1039–43.
15. Bulla R, Tripodo C, Rami D, Ling GS, Agostinis C, Guarnotta C, et al. C1q acts in the tumour microenvironment as a cancer-promoting factor independently of complement activation. Nat Commun. 2016;7:10346. https://doi.org/10.1038/ncomms10346
16. Riihilä PM, Nissinen LM, Ala-Aho R, Kallajoki M, Grénman R, Meri S, et al. Complement factor H: a biomarker for progression of cutaneous squamous cell carcinoma. J Invest Dermatol. 2014;134:498–506. https://doi.org/10.1038/jid.2013.346
17. Ajona D, Ortiz-Espinosa S, Pio R. Complement anaphylatoxins C3a and C5a: emerging roles in cancer progression and treatment. Semin Cell Dev Biol. 2019;85:153–63. https://doi.org/10.1016/j.semcdb.2017.11.023
18. Ajona D, Zandueta C, Corrales L, Moreno H, Pajares MJ, Ortiz-Espinosa S, et al. Blockade of the complement C5a/C5aR1 axis impairs lung cancer bone metastasis by CXCL16-mediated effects. Am J Respir Crit Care Med. 2018;197:1164–76.
19. Chen J, Li G, Zhang L, Tang M, Cao X, Xu G l, et al. Complement C5a/C5aR pathway potentiates the pathogenesis of gastric cancer by down-regulating p21 expression. Cancer Lett. 2018;412:30–6.

20. Zhao C, Li Y, Qiu W, He F, Zhang W, Zhao D, et al. C5a induces A549 cell proliferation of non-small cell lung cancer via GDF15 gene activation mediated by GCN5-dependent KLF5 acetylation. Oncogene. 2018;37:4821–37. https://doi.org/10.1038/s41388-018-0298-9
21. Luo L, Li X, Hu X, Hu C, Tang W, Deng S, et al. Anaphylatoxins enhance recruitment of nonclassical monocytes via chemokines produced by pleural mesothelial cells in tuberculous pleural effusion. Am J Respir Cell Mol Biol. 2019;60:454–64. https://doi.org/10.1165/rcmb.2018-0075OC
22. Hu CP, Xun QF, Li XZ, Hu XY, Qin L, He RX, et al. Effects of glucocorticoid-induced transcript 1 gene deficiency on glucocorticoid activation in asthmatic mice. Chin Med J (Engl). 2018;131:2817–26. https://doi.org/10.4103/0366-6999.246061
23. Roumenina LT, Daugan MV, Petitprez F, Sautès-Fridman C, Fridman WH. Context-dependent roles of complement in cancer. Nat Rev Cancer. 2019;19:698–715. https://doi.org/10.1038/s41568-019-0210-0
24. Li J, Li H, Yu Y, Liu Y, Liu Y, Ma Q, et al. Mannan-binding lectin suppresses growth of hepatocellular carcinoma by regulating hepatic stellate cell activation via the ERK/COX-2/PGE 2 pathway. Onco Targets Ther. 2019;8:e1527650. https://doi.org/10.1080/2162402X.2018.1527650
25. Narasimhan PB, Marcovecchio P, Hamers AAJ, Hedrick CC. Nonclassical monocytes in health and disease. Annu Rev Immunol. 2019;37:439–56. https://doi.org/10.1146/annurev-immunol-042617-053119
26. Wang F, Yang L, Gao Q, Huang L, Wang L, Wang J, et al. CD163+-CD14+ macrophages, a potential immune biomarker for malignant pleural effusion. Cancer Immunol Immunother. 2015;64:965–76. https://doi.org/10.1007/s00262-015-1701-9
27. Bin PX, Wu XZ, Yi FS, Zhai K, Shi HZ. Diagnostic value of CD206+-CD14+ macrophages in diagnosis of lung cancer originated malignant pleural effusion. J Thorac Dis. 2019;11:2730–6. https://doi.org/10.21037/jtd.2019.06.44
28. Carvelli J, Demaria O, Vély F, Batista L, Chouaki Benmansour N, Fares J, et al. Association of COVID-19 inflammation with activation of the C5a–C5aR1 axis. Nature. 2020;588:146–50. https://doi.org/10.1038/s41586-020-2600-6
29. Ajona D, Ortiz-Espinosa S, Moreno H, Lozano T, Pajares MJ, Agorreta J, et al. A combined PD-1/C5a blockade synergistically protects against lung cancer growth and metastasis. Cancer Discov. 2017;7:694–703. https://doi.org/10.1158/2159-8290.CD-16-1184
30. Kapellos TS, Bonaguro L, Gemünd I, Reusch N, Saglam A, Hinkley ER, et al. Human monocyte subsets and phenotypes in major chronic inflammatory diseases. Front Immunol. 2019;10:2035–48. https://doi.org/10.3389/fimmu.2019.02035
31. Cros J, Cagnard N, Woollard K, Patey N, Zhang SY, Senechal B, et al. Human CD14dim monocytes patrol and sense nucleic acids and viruses via TLR7 and TLR8 receptors. Immunity. 2010;33:375–86.
32. Mantovani A, Barajon I, Garlanda C. IL-1 and IL-1 regulatory pathways in cancer progression and therapy. Immunol Rev. 2018;281:57–61. https://doi.org/10.1111/imr.12614
33. Cumpelik A, Ankli B, Zecher D, Schifferli JA. Neutrophil microvesicles resolve gout by inhibiting C5a-mediated priming of the inflammasome. Ann Rheum Dis. 2016;75:1236–45. https://doi.org/10.1136/annrheumdis-2015-207338
34. Perianayagam MC, Balakrishnan VS, King AJ, Pereira BJG, Jaber BL. C5a delays apoptosis of human neutrophils by a phosphatidylinositol 3-kinase-signaling pathway. Kidney Int. 2002;61:456–63. https://doi.org/10.1046/j.1523-1755.2002.00139.x
35. Lalli PN, Strainic MG, Yang M, Lin F, Medof ME, Heeger PS. Locally produced C5a binds to T cell expressed C5aR to enhance effector T-cell expansion by limiting antigen-induced apoptosis. Blood. 2008;112:1759–66. https://doi.org/10.1182/blood-2008-04-151068
36. Hu R, Chen ZF, Yan J, Li QF, Huang Y, Xu H, et al. Complement C5a exacerbates acute lung injury induced through autophagy-mediated alveolar macrophage apoptosis. Cell Death Dis. 2014;5:e1330. https://doi.org/10.1038/cddis.2014.274
37. Miyabe Y, Miyabe C, Murooka TT, Kim EY, Newton GA, Kim ND, et al. Complement C5a receptor is the key initiator of neutrophil adhesion igniting immune complex–induced arthritis. Sci Immunol. 2017;2:2195. https://doi.org/10.1126/sciimmunol.aaj2195
38. Peng Q, Wu W, Wu KY, Cao B, Qiang C, Li K, et al. The C5a/C5aR1 axis promotes progression of renal tubulointerstitial fibrosis in a mouse model of renal ischemia/reperfusion injury. Kidney Int. 2019;96:117–28. https://doi.org/10.1016/j.kint.2019.01.039
39. Moossavi M, Parsamanesh N, Bahrami A, Atkin SL, Sahebkar A. Role of the NLRP3 inflammasome in cancer. Mol Cancer. 2018;17:158. https://doi.org/10.1186/s12943-018-0900-3
40. Hughes T, Becknell B, Freud AG, McClory S, Briercheck E, Yu J, et al. Interleukin-1β selectively expands and sustains interleukin-22+ immature human natural killer cells in secondary lymphoid tissue. Immunity. 2010;32:803–14. https://doi.org/10.1016/j.immuni.2010.06.007
41. Hübner M, Effinger D, Wu T, Strauß G, Pogoda K, Kreth FW, et al. The IL-1 antagonist anakinra attenuates glioblastoma aggressiveness by dampening tumor-associated inflammation. Cancers (Basel). 2020;12:433–47. https://doi.org/10.3390/cancers12020433
42. Guadagno J, Swan P, Shaikh R, Cregan SP. Microglia-derived IL-1β triggers p53-mediated cell cycle arrest and apoptosis in neural precursor cells. Cell Death Dis. 2015;6:e1779. https://doi.org/10.1038/cddis.2015.151
43. Mahr S, Neumayer N, Gerhard M, Classen M, Prinz C. IL-1β-induced apoptosis in rat gastric enterochromaffin-like cells is mediated by iNOS, NF-κB, and bax protein. Gastroenterology. 2000;118:515–24. https://doi.org/10.1016/S0016-5085(00)70257-5

SUPPORTING INFORMATION

Additional supporting information may be found in the online version of the article at the publisher's website.

How to cite this article: Luo L, Deng S, Tang W, Hu X, Yin F, Ge H, et al. Recruitment of IL-1β-producing intermediate monocytes enhanced by C5a contributes to the development of malignant pleural effusion. Thorac Cancer. 2022;13:811–23. https://doi.org/10.1111/1759-7714.14324